Biochimica et Biophysica Acta 809 (1985) 228–235
Elsevier

BBA 41840

Measurement of diffusion potentials in liposomes. Origin and properties of the threshold level in the oxonol VI response

K. Krab *, H.S. van Walraven, M.J.C. Scholts and R. Kraayenhof

Biological Laboratory, Vrije Universiteit, De Boelelaan 1087, 1081 HV Amsterdam (The Netherlands)

(Received March 27th, 1985)

Key words: Liposome; Diffusion potential; Membrane potential; Oxonol VI

A model is presented for the response of the membrane potential probe oxonol VI on diffusion potentials in liposomes. In this model the dependence of the probe response on the initial ion gradient is explained in terms of internal volume, internal ion concentration, membrane capacity and initial membrane potential. It is found that in the presence of an initial membrane potential (positive outside) there is a threshold value of the ion gradient needed for a probe response, which increases when the internal volume or the internal ion concentration decrease. The model is confirmed by experiments with liposomes of different sizes and internal KCl concentrations, prepared from asolectin or lipids isolated from the thermophilic cyanobacterium *Synechococcus* 6716. The significance of the model for threshold values observed in other energy-dependent phenomena is discussed.

Introduction

Oxonol VI has been one of the more succesful probes used to measure transmembrane potential differences [1–3]. Its use is limited to the measurement of membrane potentials that are negative outside [4], such as those that occur in submitochondrial particles [1] or chloroplasts [2,3] that are energized by electron transfer or ATP hydrolysis. Quantitative use of the probe depends on the possibility to calibrate the probe response. To this purpose ion-diffusion potentials (for oxonol VI: negative outside) may be used. Possibilities are valinomycin-induced K^+ influx, or uncoupler-induced H^+ influx in the presence of an appropriate $[K^+]$ or pH gradient, respectively [2,3]. In these calibrations it is assumed that the Nernst equation holds and that the ionophore-induced diffusion potential may be calculated from the initial ion concentration gradient.

The underlying assumption of the validity of the Nernst equation implies that a plot of the probe response against the logarithm of the concentration gradient used in the calibration procedure goes through the origin; without an ion gradient, the relevant ionophore should not induce a diffusion potential, and the probe should not respond. However, the calibration curve (closely approaching a straight line [2]) intersects the x-axis at a positive value of the concentration gradient. In other words, there seems to be a threshold membrane potential (negative outside) that has to be produced before the probe starts to respond.

For complicated systems like chloroplast thylakoids or submitochondrial particles, explanations for this threshold value may be given, such as a difference in activity coefficient for K^+ between both sides of the membrane [2] or, generally, lack of knowledge about the K^+ activity inside.

We are presently concerned with the measure-

* To whom correspondence should be addressed.

Abbreviation: Oxonol VI, bis(3-propyl-5-oxoisoxazol-4-yl)pentamethine oxonol.

ment of membrane potentials in relatively simply systems of liposomes reconstituted with a single protein, such as ATP synthase, respiratory chain complexes, photosynthetic electron transfer chain complexes or bacteriorhodopsin. We noticed that for a number of proteoliposome systems the threshold value for the oxonol VI response was quite variable. Therefore, we decided to investigate, in an even more simple system consisting of liposomes without incorporated protein, the factors that determine the occurrence and the magnitude of the threshold level in the oxonol VI response.

We present here a simple mathematical model that explains our results both in liposomes and proteoliposomes, and discuss its limitations. Finally, we extrapolate our conclusions to more complicated systems such as chloroplasts and submitochondrial particles, and to other energization-dependent phenomena (e.g., ATP synthesis).

Materials and Methods

Synechococcus 6716 (at 50°C) and *Synechococcus* 6301 (at 30°C) were grown as described by Lubberding et al. [5].

Lipids were isolated from these strains as described before [6].

Liposomes were prepared using each of two methods: sonication or detergent dialysis [7]. In the sonication procedure 10 mg lipid per ml medium was sonicated under a stream of nitrogen for 15 min (amplitude 4 μm) using a MSE Soniprep 150. The medium contained either 1 mM KCl with 199 mM NaCl, or 10 mM KCl with 190 mM NaCl, plus 8 mM Na-Tricine buffer (pH 7.6). Sonication was carried out on ice, except for the preparation from lipids from *Synechococcus* 6716. The dialysis procedure was carried out as described [7], in a medium containing either 1 mM or 10 mM KCl, plus 2.5 mM $MgCl_2$ and 8 mM Na-Tricine buffer (pH 7.6), at 50°C for thermophilic *Synechococcus* 6716 lipids, and at 30°C for mesophilic *Synechococcus* 6301 lipids or asolectin. The dialysis time was 24 h.

Apart from KCl concentration (and NaCl concentration in the experiments with liposomes prepared by sonication), the external media were the same as the reconstitution media.

Oxonol VI absorbance changes were measured at 625–603 nm with an Aminco DW 2a dual-wavelength spectrophotometer in either 1 cm light-path plastic disposable cuvettes (manual mixing) or in a multi-purpose cuvette [8]. Measurements were done at 50°C for liposomes from *Synechococcus* 6716 lipids and at 25°C for liposomes prepared from *Synechococcus* 6301 lipids or asolectin.

Asolectin was obtained from Associated Concentrates and purified according to Kagawa and Racker [9]. Oxonol VI was a kind gift from Prof. W. Hanstein (Ruhr-Universität Bochum, F.R.G.), and synthesized by him. Valinomycin was obtained from Boehringer (Mannheim, F.R.G.), sodium cholate from ICN Pharmaceuticals Inc. (New York, U.S.A.) and octylglucoside (*n*-octyl-β-D-glucopyranoside) from Calbiochem (La Jolla, U.S.A.).

Results

Theoretical treatment of the model system

Fig. 1. illustrates the model system consisting of two compartments containing a solution of a potassium salt, separated by a membrane. Each compartment is characterized by its volume V, the total amount of K^+ present, N (in moles) and the electrostatic potential, ψ (assumed to be homogeneous throughout the compartment). When n mol of K^+ ions are transferred from the left compartment to the right one, both the potassium ion concentrations (N_L/V_L and N_R/V_R) and the elec-

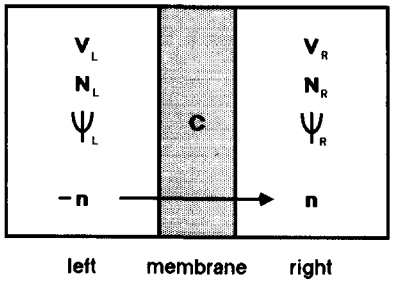

Fig. 1. Model for transmembrane diffusion potential gradients. The volumes, V, the amounts of K^+, N, and the electrostatic potentials, ψ, are labelled L or R to indicate the left and right compartments, respectively. C is the electric capacity of the membrane separating the compartments, and the arrow indicates the transfer of n mol K^+ from left to right. Further explanation in text.

trostatic potential difference $\Delta\psi = \psi_L - \psi_R$ between the compartments change. In the case of K^+ transport across the membrane, its driving force would then be:

$$\Delta\bar{\mu}_{K^+} = F\Delta\psi + RT\Delta \ln[K^+] \quad (1)$$

(Δ defined as left minus right). The changes in this expression upon transport of n mol K^+ may be calculated after some assumptions. For the $\Delta\psi$ it is assumed that the membrane behaves as a simple condensor:

$$n = -C\partial\Delta\psi \quad (2)$$

in which ∂ indicates a change, and C is a capacitance factor expressed in mol per V.

The change of the concentration term can be calculated to be equal to

$$\partial(RT\Delta \ln[K^+]) = -RT\left(\frac{1}{N_L} + \frac{1}{N_R}\right)n \quad (3)$$

(N_L and N_R refer to initial values, and to obtain an expression explicit in n, it has been assumed that $|n/N_i|$ is much smaller than unity, so that $\ln(1 \pm n/N_i)$ may be approximated by $\pm n/N_i$, i = L, R).

Let us now consider the situation in which, starting from an initial $\Delta\psi_0$ and $\Delta \ln[K^+]_0$, the membrane is made permeant for K^+ (e.g., by addition of the ionophore valinomycin). After transport of n moles K^+ an equilibrium situation is reached in which $F\Delta\psi_e = -RT\Delta \ln[K^+]_e$. From this equality and from the application of Eqns. 2 and 3 it can be calculated that the amount of K^+ transported to reach equilibrium is:

$$n = fC(F\Delta\psi_0 + RT\Delta \ln[K^+]_0)/F \quad (4)$$

in which

$$f = \frac{F}{F + RTC\left(\frac{1}{N_L} + \frac{1}{N_R}\right)} \quad (5)$$

and the final $\Delta\psi_e$ is equal to:

$$\Delta\psi_e = (1-f)\Delta\psi_0 - fRT\Delta \ln[K^+]_0/F \quad (6)$$

Fig. 2 A–C shows a schematic drawing of $\Delta\psi_e$ as a function of $\Delta \log[K^+]_0$, for $\Delta\psi_0 < 0$, $\Delta\psi_0 = 0$ and $\Delta\psi_0 > 0$, respectively (the value of $\Delta\psi_0$ is indicated by the dashed lines). To obtain the response of the probe oxonol VI upon addition of valinomycin, some assumptions about how the probe reacts on the membrane potential have been made. In the first place, the probe shows a signal (increase in the absorbance difference at 625–603 nm) only when the membrane potential is negative outside (taken to be the left side of the model) [4]. Secondly, the probe response has then been assumed to be proportional to the magnitude of the negative $\Delta\psi$. This latter assumption is not essential for what follows, but is simplifies Fig. 2.

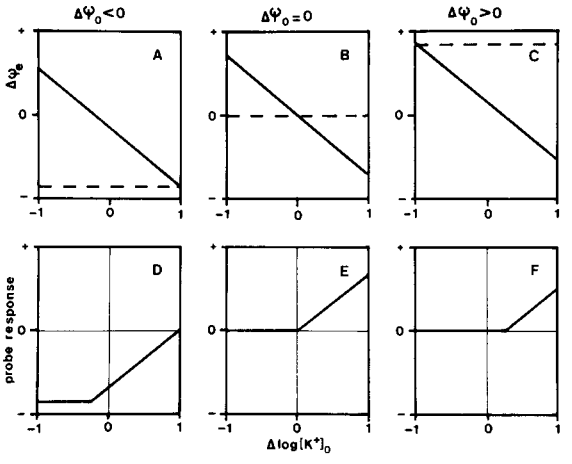

Fig. 2. Schematic drawing of valinomycin-induced membrane potential and oxonol VI response as a function of initial potassium gradient. In the upper three panels $\Delta\psi_e$ is plotted against $\Delta \log[K^+]_0$ in the cases where $\Delta\psi_0 < 0$ (A), $\Delta\psi_0 = 0$ (B) and $\Delta\psi_0 > 0$ (C). $\Delta\psi_0$ is also indicated (dashed lines). In the lower three panels, the oxonol VI response is given for $\Delta\psi_0 < 0$ (D), $\Delta\psi_0 = 0$ (E) and $\Delta\psi_0 > 0$ (F). The lines have been calculated with $f = 0.8$, and $\Delta\psi_0$ corresponding to one decade.

The probe response upon addition of valinomycin reflects the change of the membrane potential from $\Delta\psi_0$ to $\Delta\psi_e$. Hence, as illustrated in Fig. 2 D–F, this response is different in the three cases shown in Fig. 2 A–C. Thus, in the case that $\Delta\psi_0 < 0$, at low values of $\Delta \log[K^+]_0$ a negative probe response may be expected (shown in Fig. 2D). When $\Delta\psi_0 = 0$ the line giving the probe response as a function of the initial K^+ gradient goes through the origin (Fig. 2E), and when $\Delta\psi_0 > 0$ there is an x-axis intercept at $\Delta \log[K^+]_0 = F \log e\, \Delta\psi_0(1-f)/fRT$. Below the intercept the

probe response is zero (Fig. 2F). The model thus predicts an intercept, proportional to $\Delta\psi_0$, when there is a pre-existing membrane potential (positive outside).

From Eqn. 5 it can be calculated that the magnitude of the intercept depends on the properties of the system according to:

$$\text{intercept} = \Delta\psi_0 C \log e(1/N_L + 1/N_R) \quad (7)$$

When the left compartment is taken to be equal to the outside of liposomes or other small particles, the term $1/N_L$ may be neglected. Then also, $N_R = V_i\ [K^+]_i$ (in which i stands for "inside"), so that

$$\text{intercept} = \Delta\psi_0 C \log e/V_i[K^+]_i \quad (8)$$

The value of the intercept thus should be inversely proportional to the volume and the $[K^+]_i$ of the vesicles under investigation. In Table I some intercepts are given, as calculated for liposomes of 30 and 300 nm diameter, respectively (see below). Three values of $[K^+]_i$ (1, 10 and 100 mM) are used, C is calculated from the value given for the inner mitochondrial (phospholipid) membrane ([10] see also Ref. 11) and the size of the vesicles, and $\Delta\psi_0$ is arbitrarily taken to be equal to 0.06 V. It is clear that the model predicts a detectable intercept only for small vesicles.

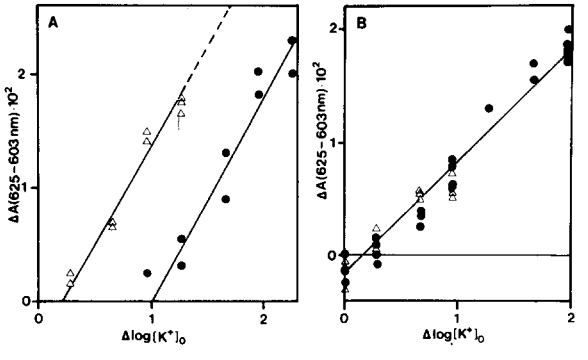

Fig. 3. Dependence of valinomycin-induced oxonol VI absorbance change in asolectin liposomes on the size of the initial K^+ gradient. (A) Liposomes prepared by sonication; (B) liposomes prepared by dialysis. △, Internal KCl concentration 10 mM; ●, internal KCl concentration 1 mM. Lipid concentration was 1 mg·ml^{-1} and 1 μM oxonol VI was present. Absorbance changes were initiated by addition of 100 nM valinomycin. The temperature was 25°C.

Diffusion potentials in asolectin liposomes

Measurement of the oxonol response in liposomes made by sonication of asolectin suspensions leads to approx. straight-line dependencies of the measured absorbance change on $\Delta\ln[K^+]_0$ that show an intercept with the positive $\Delta\ln[K^+]_0$ axis. The reactions were started by addition of 0.1 μM valinomycin to a suspension of liposomes with 1 μM oxonol VI and the appropriate external $[K^+]$ present. Fig. 3A shows an intercept of 1.0 obtained with liposomes containing 1 mM K^+ and an intercept of 0.2 with 10 mM internal K^+. When liposomes are made by the dialysis method, the calibration lines for liposomes containing 1 mM and 10 mM K^+ are identical, within experimental error, and both intercept close to the origin (Fig. 3B).

Fig. 4A shows that asolectin liposomes prepared by the dialysis technique are large and unilamellar.

The oxonol VI response in cyanobacterial lipid liposomes

Liposomes made from lipids extracted from the mesophilic cyanobacterial strain *Synechococcus* 6301 show a more complex response upon addition of valinomycin. This is illustrated in Fig. 5. Traces A and B in Fig. 5 show the effect of consecutive additions of valinomycin to asolectin liposomes. The first addition evokes a typical 'diffusion potential response'; later additions have no effect. This result is obtained with liposomes prepared by either sonication (A) or dialysis (B). Traces C and D show the same experiments with sonicated and dialyzed liposomes from *Synechococcus* 6301 lipids, respectively. Here, each addition leads to an increase of absorbance which does not decay to the initial level. This stable jump in absorbance increases with the amount of valinomycin and with outside $[K^+]$, but does not require a K^+ gradient and is not sensitive to uncoupler (further results on this matter will be dealt with elsewhere). Hence, this jump does not reflect a diffusion potential. With these liposomes we have not been able to observe a regular diffusion potential-dependent oxonol VI signal. In the case of liposomes prepared from lipids of the thermophilic *Synechococcus* 6716 this artefactual effect is absent (not shown). When these liposomes

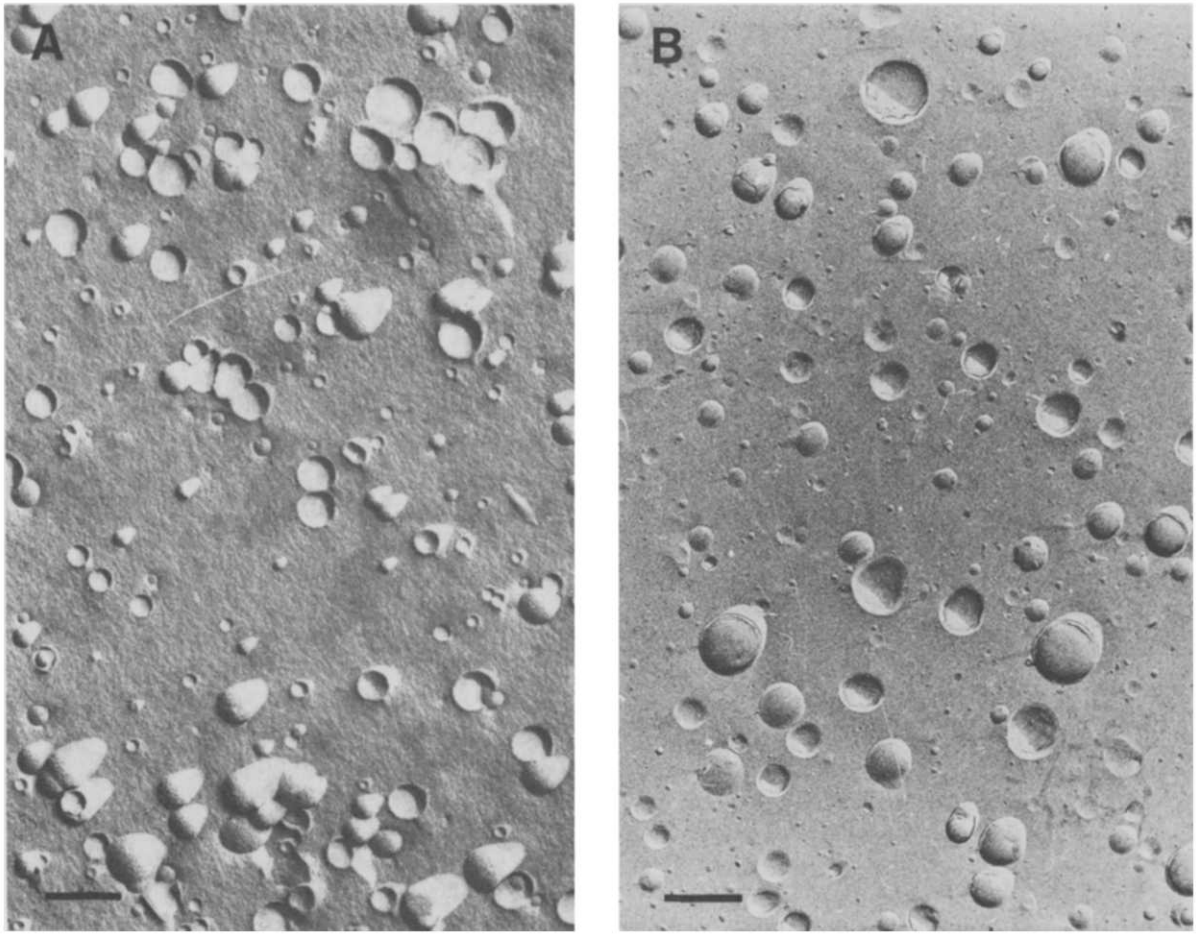

Fig. 4. Morphology of liposomes prepared by detergent dialysis. Freeze-fracture replicas of liposomal preparations were made as in Ref. 7. Asolectin liposomes were rapidly frozen in liquid nitrogen from room temperature, cyanobacterial lipid liposomes were rapidly frozen from 50°C. (A) Asolectin liposomes; (B) cyanobacterial lipid liposomes. Scale bars indicate 400 nm.

are prepared by sonication a valinomycin-induced oxonol response identical to that in asolectin liposomes is observed (Fig. 5, trace E). However, in liposomes prepared from thermophilic lipids by the dialysis technique, the rise of the oxonol signal after valinomycin addition is slower (takes about 2 min, see Fig. 5, trace F). The final level is then extremely stable (at least 30 min). The same oxonol response has been observed in ATPase proteoliposomes prepared from these lipids by the same technique [14].

When the maximal extent of the probe response in sonicated thermophilic lipid liposomes is plotted as a function of the initial K^+ gradient the same result is obtained as with sonicated asolectin liposomes: a significant x-axis intercept, which increases when the internal K^+ concentration decreases (Fig. 6A). The points given at zero initial gradient indicate a negative response. However, this response is kinetically different from the positive responses of the probe obtained at positive values of $\Delta \ln[K^+]$ and reflects a slow absorbance decrease, the origin of which we do not yet understand (not shown).

When the absorbance levels reached with the dialyzed lipid liposomes are plotted against the initial K^+ gradient, a line going almost through the origin is found (Fig. 6B), again in fair agree-

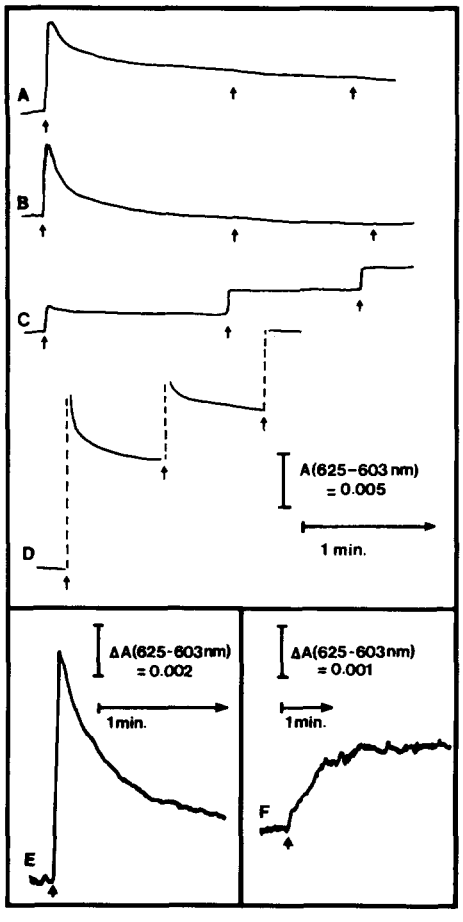

Fig. 5. Time-course of oxonol VI response upon valinomycin addition in different types of liposomes. (A) Asolectin liposomes prepared by sonication, internal K^+ 1 mM, external K^+ 200 mM; (B) asolectin liposomes prepared by dialysis, internal K^+ 1 mM, external K^+ 200 mM: (C) mesophilic lipid liposomes prepared by sonication, internal K^+ 10 mM, external K^+ 200 mM; (D) mesophilic lipid liposomes prepared by dialysis, internal K^+ 1 mM, external K^+ 200 mM; (E) thermophilic lipid liposomes prepared by sonication, internal K^+ 10 mM, external K^+ 200 mM (F) thermophilic lipid liposomes prepared by dialysis, internal K^+ 10 mM, external K^+ 100 mM. Arrows indicate additions of 100 nM valinomycin. Either 1 μM (A–D) or 0.5 μM (E,F) oxonol VI was present. Final lipid concentration was 1 mg·ml^{-1} (A–D), 0.5 mg·ml^{-1} (E) or 0.25 mg·ml^{-1} (F). Temperature was 20°C (A–D) or 50°C (E,F).

ment with the results obtained with dialyzed asolectin liposomes. Fig. 4B shows that also those liposomes prepared by the dialysis technique from cyanobacterial lipid are large and unilamellar.

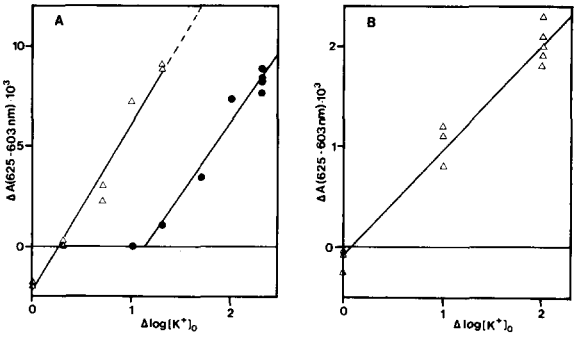

Fig. 6. Dependence of valinomycin-induced oxonol VI absorbance change in thermophilic lipid liposomes on the size of the initial K^+ gradient. (A) Liposomes prepared by sonication; (B) liposomes prepared by dialysis. △, internal KCl concentration 10 mM; ●, 1 mM. 0.5 μM oxonol VI was present and final lipid concentration was 0.5 mg·ml^{-1} (A) or 0.25 mg·ml^{-1} (B). Temperature was 50°C.

Discussion

The model presented gives a qualitative fit to the results obtained with asolectin liposomes. It predicts correctly the absence of an intercept ('threshold level' for the diffusion potential) with the large dialysis liposomes, and the presence of an intercept with the small sonicated liposomes, the size of which decreases when the initial $[K^+]$ increases. Liposomes obtained by dialysis have diameters of 100–300 nm (fig, 4, and c.f. Refs 7 and 12), whereas liposomes prepared by sonication are 20–50 nm in diameter [13]. The quantitative fit, however, is less satisfactory. Comparison between the experimental results of Figs 3 and 6 and the predictions in Table I shows that the difference in intercept between sonicated liposomes with 1 mM and 10 mM internal $[K^+]$ is slightly smaller than expected. Eqn. 8 predicts a 10-fold change of the intercept when the internal $[K^+]$ is changed by a factor of 10, while the change measured is roughly a factor 5. The model also predicts a difference in the slope of the calibration lines for these two types of liposome (see Eqn. 6 and Table I). However, such a difference in the experimental results is hard to assess due to the uncertainty about the 'extinction coefficient' relating the probe response to $\Delta\psi_e$ in the different vesicle preparations.

There are several assumptions underlying the model that may be the basis for the quantitative

TABLE I

SLOPES AND INTERCEPTS OF PLOTS OF $\Delta\psi_e$ VS. $\Delta[K^+]$

The calculations were done with a membrane capacity of 0.01 $C \cdot V^{-1} \cdot m^{-2}$ [10] and a membrane thickness of 6 nm, and assuming the liposomes to be spherical. For the calculation of the intercept, $\Delta\psi_0$ was arbitrarily taken to be 0.06 V. For factor f, see equation 5.

Diameter of liposomes (nm)	$[K^+]_i$ (mM)	f	slope ($mV \cdot unit^{-1}$)	X-axis intercept
30	1	0.3879	−23	1.60
30	10	0.8637	−51	0.16
30	100	0.9845	−58	0.02
300	1	0.9454	−56	0.06
300	10	0.9943	−59	0.01
300	100	0.9994	−59	0.00

discrepancies. Firstly, it has been assumed that macroscopic thermodynamics apply (use of Eqn 1, and the relationship between $\Delta\psi$ and $\Delta \ln[K^+]$ at equilibrium) and that surface phenomena may be neglected (homogeneous ψ throughout the compartments). Secondly, it has been assumed that the electric properties of the liposomal membrane may be approximated by Eqn 2. It is known [15,16] that at high values of $\Delta\psi$ the conductance of liposomal membranes increases, but some indication that this effect does not interfere here may be derived from the shape of the lines in Figs. 3 and 6. The third assumption is the mathematical approximation used in the derivation of Eqn. 3. Using Eqn. 6 it can be easily calculated that for small sonicated liposomes with 1 mM internal K^+ n/N_R is quite large. This will detract from the quantitative fit of the model, especially in cases where large intercepts are expected.

However, the main feature of the model, the correlation between internal volume and K^+ concentration with the shape of the calibration curve, is substantiated by the results, both with asolectin liposomes and with *Synechococcus* 6716 lipid liposomes. In this respect, it is interesting to note that the compositions of the two kinds of lipid mixture are quite different. Asolectin is mainly composed from charged lipids (phosphatidylethanolamine, phosphatidylcholine, phosphatidylserine and some cardiolipin, see e.g. Ref. 17), whereas the cyanobacterial lipids mainly contain galactolipids, sulfoquinovosyl diacylglycerol and phosphatidylglycerol [6].

In addition, completely consistent results have been obtained with dialyzed proteoliposomes reconstituted from ATP synthase complex and lipids from the thermophilic cyanobacterial strain *Synechococcus* 6716 [14] and with sonicated asolectin liposomes reconstituted with bacteriorhodopsin or with bacteriorhodopsin and yeast mitochondrial ATP synthase (Van Walraven and Van de Bend, unpublished results).

The model explains the intercepts as a consequence of the existence of an initial membrane potential $\Delta\psi_0$. This $\Delta\psi_0$ may be caused by asymmetric distribution of surface charge (lipid head groups) on both sides of the liposomal membrane. As a consequence of this, $\Delta\psi_e$ has to reach a certain value to compensate the surface potential to enable oxonol to respond. Also, the mechanism of the oxonol VI response itself could involve the requirement of a threshold value. However, a threshold of this type alone would not lead to the observed results. Eqn. 6 predicts that in the absence of an initial membrane potential ($\Delta\psi_0 = 0$) $\Delta\psi_e$ should be proportional to f, and thus the intercept in the plot of probe response against initial K^+ gradient should be proportional to $1/f$. From Table I it may be inferred that this should result in a much smaller difference between the calibration lines for sonicated and dialyzed lipids (roughly a factor 2).

If the threshold level in the calibration lines does not derive from the properties of the probe, it should also occur, with the same dependence on vesicle size, in other energy-dependent phenomena. Indeed, ATP synthesis driven by K^+ influx shows a large threshold in small proteoliposomes [18], and a small threshold in large dialyzed proteoliposomes [14].

In chloroplasts, high threshold values for ΔpH-induced ATP synthesis are found which may be overcome by a K^+ diffusion potential [19,20]. Uribe [21] has shown that ATP synthesis driven by a K^+ gradient plus valinomycin alone (with external $[K^+]$ up to 40 mM) may be observed in chloroplasts isolated in hypotonic medium, but not in chloroplasts isolated in isotonic medium. This difference could be caused by a smaller amount of K^+ available in the smaller osmotic volume of the

second type of chloroplasts. Threshold values in chloroplasts are generally explained as due to activation of the ATP synthase complex [22]; however, a basal membrane potential as in the model may also be contributing to the threshold. An additional complication in the interpretation of the results obtained with chloroplasts is the uncertainty about ion activities in the chloroplast lumen. For the same reason, interpretation of the threshold in the oxonol response obtained with chloroplasts [2] is difficult.

Acknowledgments

We would like to thank Mrs. J. Leunissen-Bijvelt (Department of Molecular Cell Biology, State University, Utrecht, The Netherlands) and Mr. E. Koppenaal for performing the electron microscopy, and Mr. E.J. Hotting for critical discussions. This work is supported in part by the Foundation for Biophysics and by the Netherlands Foundation for Chemical Research (SON) with financial aid from the Netherlands Organization for the Advancement of Pure Research (ZWO).

References

1 Bashford, C.L. and Thayer, W.S. (1977) J. Biol. Chem. 252, 8459–8463
2 Schuurmans, J.J., Casey, R.P. and Kraayenhof, R. (1978) FEBS Lett. 94, 405–409
3 Admon, A., Shahak, Y. and Avron, M. (1982) Biochim. Biophys. Acta 681, 405–411
4 Van Walraven, H.S., Krab, K., Hagendoorn, M.J.M. and Kraayenhof, R. (1985) FEBS Lett. 184, 96–99
5 Lubberding, H.J., Offerijns, F., Vel, W.A.C. and De Vries, P.J.R. (1981) in Photosynthesis II. Electron Transport and Photophosphorylation (Akoyunoglou, G., ed.), pp. 779–788, Balaban International Science Services, Philadelphia
6 Van Walraven, H.S., Koppenaal, E., Marvin, H.J.P., Hagendoorn, M.J.M. and Kraayenhof, R. (1984) Eur. J. Biochem. 144, 563–569.
7 Van Walraven, H.S., Lubberding, H.J., Marvin, H.J.P. and Kraayenhof, R. (1983) Eur. J. Biochem. 137, 101–106
8 Kraayenhof, R., Schuurmans, J.J., Valkier, L.J., Veen, J.P.C., Van Marum, D. and Jasper, C.G.G. (1982) Anal. Biochem. 127, 93–99
9 Kagawa, Y. and Racker, E. (1971) J. Biol. Chem. 246, 5477–5487
10 Mitchell, P. (1968) in Chemiosmotic Coupling and Energy Transduction, Glynn Research Ltd., Bodmin
11 Haydon, D.A. (1968) in Membrane Models and the Formation of Biological Membranes (Bolis, L. and Pethica, B.A., eds.), pp. 91–97, North-Holland Publishing Company, Amsterdam
12 Schwendener, R.A., Asanger, M. and Weder, H.G. (1981) Biochem. Biophys. Res. Commun. 100, 1055–1062
13 Szoka, F. and Papahadjopoulos, D. (1981) in Liposomes: From Physical Structure to Therapeutic Applications (Knight, C.G., ed.), pp. 51–82, Elsevier/North-Holland Biomedical Press, Amsterdam
14 Van Walraven, H.S., Hagendoorn, M.J.M., Krab, K., Haak, N.P. and Kraayenhof, R. (1985) Biochim. Biophys. Acta 809, 236–244
15 O'Shea, P.S., Petrone, G., Casey, R.P. and Azzi, A. (1984) Biochem. J. 219, 719–726.
16 Krishnamoorthy, G. and Hinkle, P.C. (1984) Biochemistry 23, 1640–1645
17 Casey, R.P. (1984) Biochim. Biophys. Acta 768, 319–347
18 Admon, A. and Avron, M. (1984) EBEC Rep. 3A, 289–290
19 Schuldiner, S., Rottenberg, H. and Avron, M. (1972) FEBS Lett. 28, 173–176
20 Schuldiner, S., Rottenberg, H. and Avron, M. (1973) Eur, J. Biochem. 39, 455–462
21 Uribe, E.G. (1973) FEBS Lett. 36, 143–147
22 Gräber, P., Schlodder, E. and Witt, H.T. (1977) Biochim. Biophys. Acta 461, 426–440